

# Optimal trajectory design for higher-dimensional encoding

Kelvin J. Layton<sup>1</sup>, Feng Jia<sup>2</sup>, and Maxim Zaitsev<sup>2</sup>

<sup>1</sup>Department of Electrical and Electronic Engineering, The University of Melbourne, Melbourne, Victoria, Australia, <sup>2</sup>Dept. of Radiology, Medical Physics, University Medical Center Freiburg, Freiburg, Germany

**TARGET AUDIENCE** Researchers with an interest in trajectory design or nonlinear spatial encoding.

**PURPOSE** Spatial encoding magnetic fields (SEMs) that vary nonlinearly over the field-of-view have the potential to accelerate image acquisition and overcome safety limitations<sup>1,2</sup>. Recent work has demonstrated that the spatially varying resolution, characteristic of this type of encoding, can be controlled with combinations of linear and nonlinear fields with an appropriate trajectory<sup>3</sup>. In addition to challenging reconstruction<sup>4</sup>, trajectory design for these systems is difficult since the familiar k-space is insufficient to represent the higher dimensional encoding space. To date, trajectories have been designed based on traditional sampling schemes such as Cartesian<sup>1</sup>, radial<sup>2,3</sup> or EPI<sup>5</sup>. Trajectories based on optimizing spatial bases have also been proposed<sup>6</sup>. In this work, we propose a method to optimize the trajectory based on the theoretical variance of the reconstructed image.

**THEORY** The measurements from a single readout can be written in matrix form as  $\mathbf{y}_k = E(\theta_k)\mathbf{x}$ , where  $\mathbf{y}_k$  is a vector of measurements from the  $k^{\text{th}}$  readout,  $\mathbf{x}$  is the object's magnetization and  $E$  is the encoding matrix dependent on the trajectory parameters,  $\theta_k$ . Based on a recursive Bayesian reconstruction scheme<sup>7</sup>, the covariance of the reconstructed pixels, denoted  $P_k$ , decreases by including the  $k^{\text{th}}$  readout according to Eq. (1).

$$P_{k+1}(\theta_k) = P_k - P_k E(\theta_k)' (E(\theta_k) P_k E(\theta_k)' + \Sigma)^{-1} E(\theta_k) P_k \quad (1) \quad \min_{\theta_k} \max_i [P_{k+1}(\theta_k)]_{i,i} \quad (2)$$

In the equations above, the dash represents conjugation,  $\Sigma$  the measurement covariance and  $[P_{k+1}]_{i,i}$  denotes the  $i^{\text{th}}$  diagonal element of  $P_{k+1}$ , which is the variance of the  $i^{\text{th}}$  pixel. The optimization in Eq. (2) provides a method for automated trajectory design by selecting the parameters,  $\theta_k$ , that minimize the reconstruction variance. Each optimization step determines the next readout based on information obtained from previous readouts.

**METHODS** We considered trajectories that control four SEMs ( $x, y, x^2 - y^2, 2xy$ ) and assumed constant gradients for each readout. In this case, the trajectory during a readout is parameterized by the currents driving the SEM coils,  $\theta_k = [w_1, w_2, w_3, w_4]$ . A key idea to keep to the computation of Eq. (1) feasible is that the variance of a low-resolution reconstruction is an indicator of the performance of a high-resolution reconstruction<sup>8</sup>. At each step, the optimization algorithm calculated the variance of a  $32 \times 32$  reconstruction for 500 randomly generated parameter combinations. The final trajectory contained 64 readouts with 128 samples per readout. We set  $P_0 = I$  and  $\Sigma = \sigma^2 I$ , where  $I$  is the identity matrix and  $\sigma$  was set to 5% of the mean phantom intensity. Eight receive coils were used with RF profiles calculated from the Biot-Savart law. Measurements from each coil were simulated from a numerical phantom (Fig. 2a). Images were reconstructed to a  $128 \times 128$  matrix using a conjugate gradient algorithm. Image quality was assessed qualitatively and quantified with mean square error (MSE) between the reconstruction and the numerical phantom.

**RESULTS** Fig. 1 displays the maximum pixel variance as successive readouts are included in the reconstruction. The variance from a trajectory consisting of projections randomly selected (dashed line) is approximately three times larger than the variance from an optimally designed trajectory (solid line). The image reconstructed from simulated data using the random projections has reconstruction artifacts and increased noise (Fig. 2b) compared to the image from the optimal trajectory (Fig. 2c). Fig. 2b also exhibits a loss in resolution due to the inherent regularization of iterative reconstruction algorithms, which decrease the variance at the expense of resolution. The improvement of the optimal trajectory is particularly pronounced in the center of the field-of-view where coils sensitivities are small (Fig. 2d,e). The MSE of the images from the random and optimal trajectories are 7.4 and 4.3, respectively.

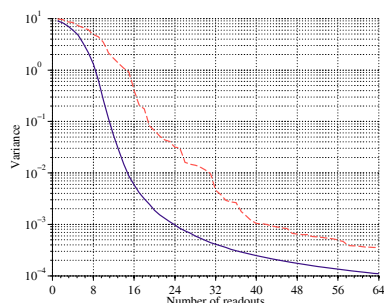


**Fig. 1** Variance of the reconstructed pixels for a trajectory based on random projections (dashed) and optimal projections (solid)

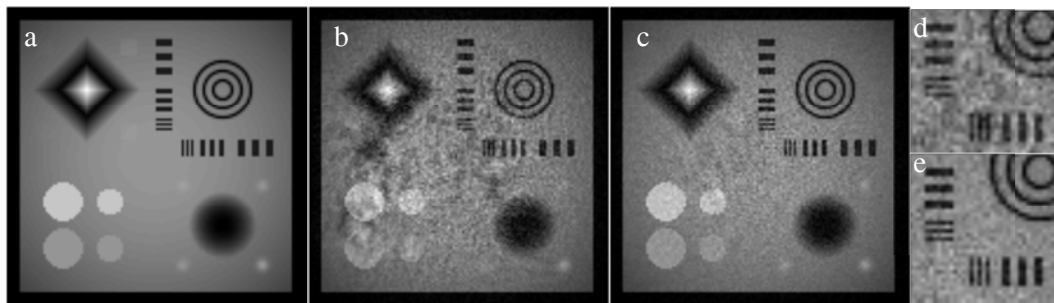


**Fig. 2** (a) Numerical phantom used for simulations and (b) reconstruction of data generated from a trajectory with encoding fields chosen at random and (c) reconstruction of data generated from an optimal trajectory. Magnified regions in (d) and (e) are from the central regions of (b) and (c), respectively.

**CONCLUSION** This work has presented a method for optimized trajectory design based on the theoretical variance of each pixel. The method explicitly considers the condition of the reconstruction problem during trajectory design. In this way it improves on methods using heuristic notions or intuition gained from local k-space<sup>3,9</sup>. These proof-of-principle simulations justify further investigations into the application of trajectory optimization for nonlinear encoding fields, such as those currently under development<sup>10</sup>.

**REFERENCES** <sup>1</sup>Schultz et al. 2010 MRM 64:1390–1403 <sup>2</sup>Stockmann et al. 2010 MRM 64:447–456 <sup>3</sup>Gallichan et al. 2011 MRM 65:702–714 <sup>4</sup>Schultz et al. 2013 MRM (early view) <sup>5</sup>Layton et al. 2013 MRM 70:684–696 <sup>6</sup>Lin F-H 2013 MRM 70:86–96 <sup>7</sup>Challa et al. 2011 Cambridge University Press <sup>8</sup>Layton et al. 2012 IEEE TMI 31:391–404 <sup>9</sup>Gallichan et al. 2012 MAGMA 25:419–431 <sup>10</sup>Jia et al. 2013 ISMRM p. 666

**ACKNOWLEDGEMENTS** This work was in part supported by European Research Council (ERC) grant 282345 'RANGEmri'